World Cancer Research Journal WCRJ 2023; 10: e2566

SNAIL PROTEIN INHIBITION BY DRUG REPOSITIONING FOR RECURRENT BREAST CANCER: AN *IN-SILICO* STUDY

M. BENGUELLA-BENMANSOUR[1,2], S.A. CHERRAK[1,3], M. DALI-SAHI[1,4]

[1]Department of Biology, University of Tlemcen, Tlemcen, Algeria
[2]Physico-Chemistry, Synthesis and Biological Activity Laboratory, University of Tlemcen, Tlemcen, Algeria
[3]Physiology, Pathophysiology and Biochemistry of Nutrition Laboratory, University of Tlemcen, Tlemcen, Algeria
[4]Analytical Chemistry and Electrochemistry Laboratory, University of Tlemcen, Tlemcen, Algeria

Abstract – *Objective:* *Snail is a transcription factor that promotes epithelial-mesenchymal transition (EMT) and facilitates tumor progression and metastasis in breast cancer. Therefore, it is a promising target for the development of anticancer agents. The objective of this study was to identify FDA-approved drugs that can be repurposed as Snail inhibitors.*

Materials and Methods: *Using a virtual screening strategy, three molecules were selected among 1615 (Stivarga, Paritaprevir and Sorafenib). Molecular docking and molecular dynamics simulation were performed to examine Snail-drugs interactions.*

Results: *Our docking analysis identified Stivarga and Sorafenib, two antineoplastic drugs, as potential repositioning drugs to treat recurrent breast cancer due to their low free binding energy values. Additional molecular dynamics simulations of the Snail-drug systems revealed that Sorafenib was the most stable, lasting from 30 to 120 ns and forming 2-4 hydrogen bonds.*

Conclusions: *The antineoplastic drugs Stivarga and Sorafenib have better affinity and inhibition of Snail and could be a simple drug therapy for recurrent breast cancer.*

KEYWORDS: *Snail, Breast cancer, Drug repositioning, Molecular docking, MD simulations.*

INTRODUCTION

The therapeutic strategy for breast cancer involves several types of treatment including surgery, radiotherapy, chemotherapy, hormone therapy and targeted therapies[1,2]. Advancements in these treatments have significantly improved patients' chances of survival. However, disease recurrence remains a major concern[3] with 15 to 20% of patients experiencing a recurrence within 10 years of their diagnosis of early breast cancer with distant metastatic disease responsible for 20 to 30% of deaths[4,5].

Various mechanisms leading to cancerous metastasis have been elucidated, the key event of which is the epithelial-mesenchymal transition (EMT)[6,7]. Regulation of this process is mediated by several transcription factors (Slug, Snail, ZEB1/2, Twist1/2, etc.) that bind to regulatory regions of target genes whose expression determines the phenotype(s) EMT and, their neoplastic progression[8].

The zinc finger proteins of Snail family, Snail/SNAI1 and Slug/ SNAI2, are transcriptional repressors[9-12]. These proteins contain a C-terminal region involved in protein binding to promoters of the target gene containing the E-box sequence. The N-terminal region contains the SNAG domain which is necessary for transcriptional repression and can bind methyltransferases and histone deacetylases[13-15].

DOI: 10.32113/wcrj_20235_2566

Corresponding Author: M. Benguella-Benmansour, PhD; e-mail: b_meriem74@yahoo.fr

There are two sites of phosphorylation of Snail by Glycogen synthase kinase-3β (GSK-3β): one controls the proteolysis of the protein in the proteasome, and the other determines its intracellular localization[16,17]. Both phosphorylated and dephosphorylated forms of Snail protein can bind to the ubiquitin ligase FBXL14, leading to its proteasomal degradation. However, DUB3 deubiquitinase prevents Snail degradation in the proteasome, thereby stabilizing it in the nucleus[18]. This involves protein kinase PAK1 which phosphorylates Snail at serine residue 246. In turn, phosphorylation of Snail at serine 11 and 92 by protein kinase A (PKA) enhances its transactivation[19].

In breast cancer cells, there is a strong expression of Slug (36%), Snail (62%) and N-cadherin (77%), while expression of E-cadherin is increased in only 20% of the cases[20]. According to Cao et al[21], high expression of Snail and low level of E-cadherin correlate with the number of breast cancer metastases in the lymph nodes[21].

In addition to their role in tumor cell invasion and metastasis, Snail proteins are also involved in resistance to genotoxic anticancer drugs. This resistance is due to their anti-apoptotic effects, ability to decrease proliferation, and ability to cause multi-drug resistance[22].

The role of Snail and Slug in tumor cell drug resistance is associated with repression of the pro-apoptotic protein genes PUMA, ATM, PTEN, p53, BID and caspase-6[23,24].

Therefore, Snail family proteins may directly participate in the development of drug resistance and the suppression of antitumor immunity. Snail's involvement in EMT indicates a need for pharmacological inhibition of these proteins[25].

Moreover, the involvement of snail in signaling pathways opens a new era in the search for new approaches in chemotherapy. Direct pharmacological inhibition is hampered by the complexity of targeting the functional domain of the protein. However, after synthesizing a Co(III) complex conjugated to a CAGGTG hexanucleotide, Vistain et al[26] proposed the E-box, a Snail binding site, as a target. Once inside the cell, the Co(III)–E-box complex attaches to Snail and prevents any interaction with DNA[26]. This has considerably reduced the invasive potential of tumor cells, suggesting that this compound will be very effective as a therapeutic inhibitor of tumor progression and metastasis in breast cancer.

Currently, the search for naturally occurring EMT inhibitors is booming due to their low toxicity to non-tumor tissues, as well as their anticarcinogenic properties[27,28].

The objective of this study is to identify drug candidates targeting the Snail protein to prevent and suppress the reappearance of breast cancer, using an *in-silico* approach.

MATERIALS AND METHODS

Ligand and protein preparation

The three-dimensional structure of co-crystallized Snail protein (PDB id: 3w5k) as reported by Choi et al[11], was obtained from Protein Data Bank (https://www.rcsb.org/). The retrieved structure shows no mutation with a resolution of 2.6 Å.

A library of 1615 structures was retrieved from the ZINC In Man dataset (FDAapproved, withdrawn, and experimental drugs) from subsets of the ZINC15 database (University of California, San Francisco, CA, USA)[29] (https://zinc15.docking.org).

Virtual screening

In order to search potentials inhibitors of Snail protein, a virtual screening was realized with PyrX tool[30,31]. Thus, we performed molecular docking using 3w5k protein as a receptor and 1615 structures from ZINC 15 database as ligands. AutoDock Vina was used for the best ligands affinity. Twelve compounds were selected with the best performance in the consensus docking protocol. The Discovery Visualizer software was used to visualize the 2D interaction diagrams.

Molecular dynamics

Molecular dynamics simulations were performed to evaluate the folding, stability, conformational changes, and dynamic behaviour of the most interesting ligands that interacted with the 3w5k protein using GROMACS 5.1.5 package with CHARMM36 force field installed on Linux system[32,33]. The protein topology was prepared with the pdb2gmx tool. The protein complexes were solvated in a triclinic box with a minimal margin of 1.0 Å from any edge to any protein atom. During simulations, all systems were solvated using the TIP3 water model, followed by addition of 12 Cl^- counterions to neutralize the system. Temperature was set equal to 300K and kept constant inside the box adopting an optimized Berendsen thermostat temperature coupling technique; the vrescale. To maintain a pressure of 1 bar during NPT equilibration, we utilized the Parrinello-Rahman pressure coupling method. A time gap of 2 fs for the overall temperature and pressure is used in order to stabilize the system. To minimize the system energy and reduce steric clashes, we used the steepest descent algorithm[34] with a maximum of 50,000 iteration steps and a cut-off of 1000 kJ/mol. The long-range electrostatics interactions are covered using Particle mesh Ewald (PME). The MD simulations continued for 120 ns at every 2-fs step.

Trajectory snapshots were taken every picosecond for the structural analysis using various GROMACS analysis tools. Root mean square deviation (RMSD) and the root mean square fluctuations (RMSF) of protein were analyzed with gmx rms, and gmx rmsf tools. The gmx hbond tool and the gyrate tool were respectively used to analyse hydrogen bonds and radius of gyration. Finally, Grace Software was used for preparing plots.

RESULTS

Molecular docking

We performed molecular docking using Snail protein (PDB id: 3w5k) as receptor and 1615 FDA approved molecules from ZINC 15 Database as ligands.

The 3w5k protein is a 264 amino acid sequence with a high conserved C terminal region that includes four zinc fingers extended from F154 to K253, responsible in the interaction of the protein with E-box sequence of the target gene promoters[35] (Figure 1).

Docking analysis provided several configurations that were scored to determine favorable binding modes. The binding free energies for 12 selected compounds with the highest docking scores are summarized in Table 1. The three retained molecules are Stivarga, Paritaprevir, and Sorafenib due to their low free energy binding for the Snail protein -9.1, -9.1 and -8.2 kcal.mol^{-1} respectively as well as their interesting therapeutic effect.

However, the Dihydroergotamine and the digoxin were not considered in this study because of their side effects despite they depicted a good free binding energy (-8.7 and -8.6 kcal/mol).

The three selected molecules belong to different classes of drugs. They were retained to be repositioned, on the basis of their strong binding energy, and also their no major adverse effects. These drugs are currently approved by the market with different indications. The Stivarga (Regorafenib) (Bayer Healthcare SAS, Loos, France), is indicated as monotherapy for the treatment of adult patients with metastatic colorectal cancer (mCRC) who have been treated previously or who

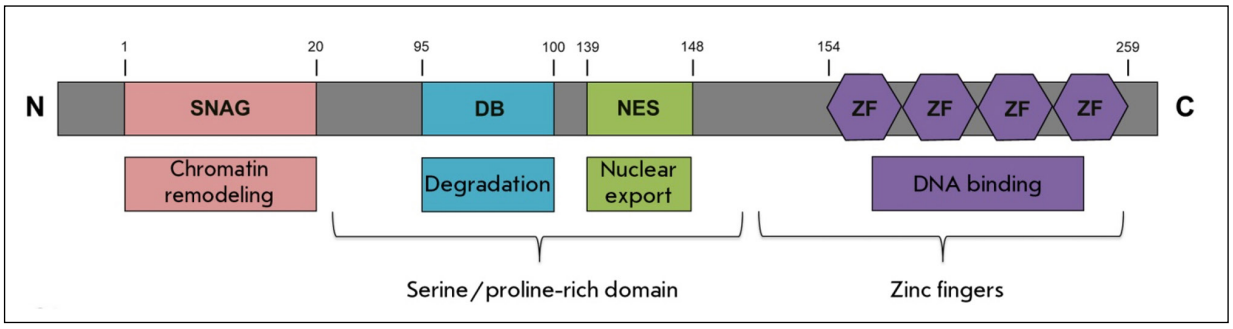

Fig. 1. Schematic representation of Snail protein (Yastrebova et al., 2020).

TABLE 1. Binding energies of retained docked compounds.

Ligands	*Zinc Code*	*Chemical formula*	*Molecular weight (g/mol)*	*ΔG (kcal/mol)*
Stivarga	6745272	$C_{21}H_{15}ClF_4N_4O_3$	482.8	-9.1
Paritaprevir	669678887	$C_{40}H_{43}N_7O_7S$	765.9	-9.1
Dihydroergotamine	3978005	$C_{33}H_{37}N_5O_5$	583,677 4	-8.7
Digoxine	242548690	$C_{41}H_{64}O_{14}$	780.949	-8.6
Ledipasvir	150338819	$C_{49}H_{54}F_2N_8O_6$	889	-8.3
Sorafenib	1493878	$C_{21}H_{16}ClF_3N_4O_3$	464.8	-8.2
Irinotecan	1612996	$C_{33}H_{38}N_4O_6$	586,678	-8.2
Olaparib	40430143	$C_{24}H_{23}FN_4O_3$	434,462 8	-8
Epinastine	1999487	$C_{16}H_{15}N_3U$	249.31	-8
Telmisartan	1530886	$C_{33}H_{30}N_4O_2$	514,616 9	-8
Lomitapide	27990463	$C_{39}H_{37}F_6N_3O_2$	693,720 4	-7.9
Atacand	3782818	$C_{24}H_{20}N_6O_3$	440,454	-7.6

are not eligible for available treatments[36]. It is also indicated for resectable or metastatic gastrointestinal stromal tumors (GIST) and hepatocellular carcinoma (HCC) which have been previously treated with Sorafenib[37]. Regorafenib is a small molecule that inhibits multiple membrane-bound and intracellular kinases involved in normal cellular functions and pathologic processes, such as tumor angiogenesis, metastasis, oncogenesis, and tumor immunity[36]. Sorafenib is a dual-action inhibitor that targets the RAF/MEK/extracellular signal-regulated kinase (ERK) pathway in tumor cells and tyrosine kinases VEGFR/PDGFR in tumor vasculature. Sorafenib was developed as an inhibitor of C-RAF kinase using a combination of medicinal and combinatorial chemistry approaches. The antiproliferative activity of Sorafenib is variable in different tumor types and largely depends on the oncogenic signaling pathways that mediate tumor proliferation. Sorafenib has also been shown to induce apoptosis in several tumor cell lines[38].

The work of Lesch et al[39] suggests that Regorafenib and Sorafenib are promising drug candidates for therapy directed against viral infections due to their effective inhibitory effects against early viral replication of the cell cycle life of human primary respiratory cells and their low cytotoxicity[39].

Paritaprevir (also known as ABT-450) is an inhibitor [identified by AbbVie (North Chicago, IL, USA) and Enanta Pharmaceuticals (Watertown, MA, USA)] of the HCV NS3-4A protease which is required for the proteolytic cleavage of the HCV encoded polyprotein and which is essential for viral replication[40]. Paritaprevir is used, in combination with ombitasvir and ritonavir, in the management of hepatitis C[41,42]. Paritaprevir, currently approved for hepatitis C treatment, which showed some of the lowest free binding energy values, was also considered as a potential repositioning drug against SARS-CoV-2[43].

As shown in Figure 2, from the molecular docking studies, we could observe that the Stivarga (a) and Sorafenib (b) showed similar binding modes in the binding pocket of 3w5k protein, due to their common chemical moieties. However, Paritaprevir (c) binds to the Snail protein in a different site as shown in Figure 2.

Discovery studio visualizer was used for interactions that governed drug-target binding. Hydrogen bonds and hydrophobic interaction (π-alkyl/alkyl) are the predominant occurring interaction between molecules (Figure 3).

Results (Figure 3) show that compounds that undertake bonds with the highest strength usually involved the Thr201, Ser209, His212, Pro207 of the structure for Stivarga (a) and Arg200, Thr203,

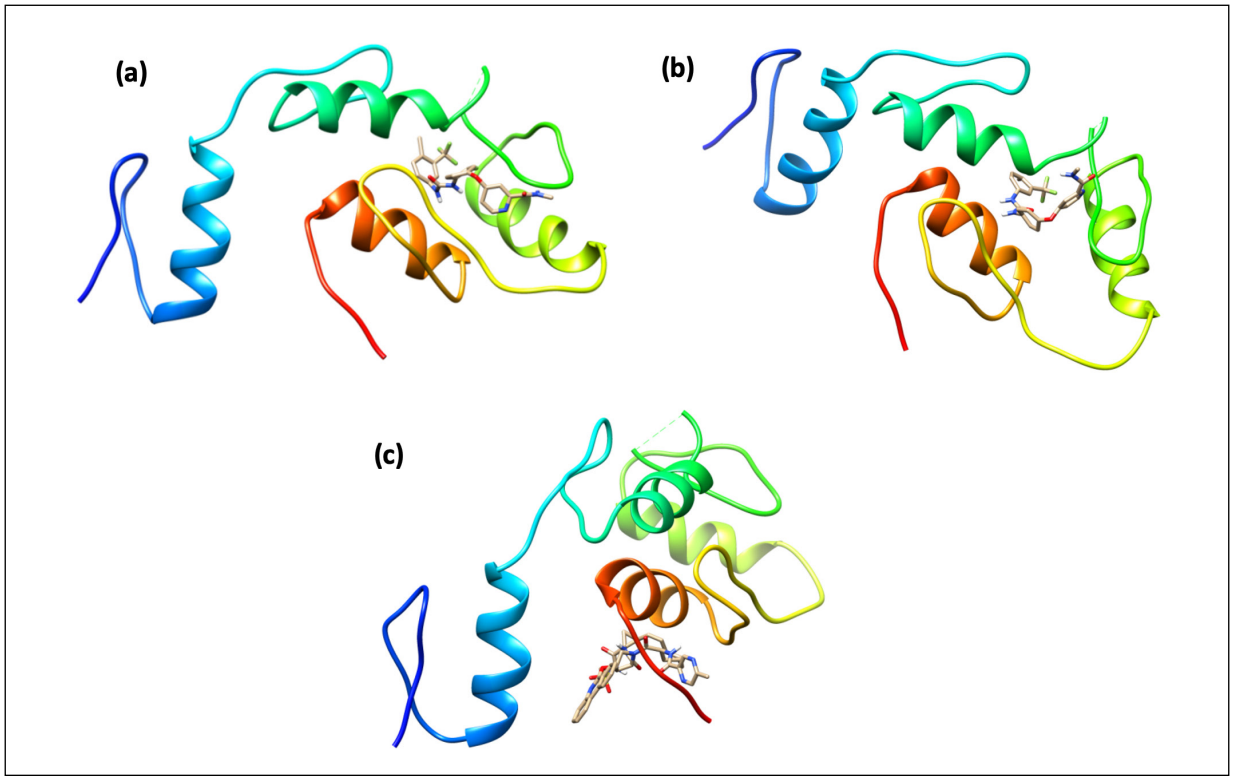

Fig. 2. Binding poses of the 3 selected compounds by virtual screening obtained by molecular docking simulations against 3w5k snail protein: Stivarga **(a)**, Sorafenib **(b)** and Paritaprevir **(c)**.

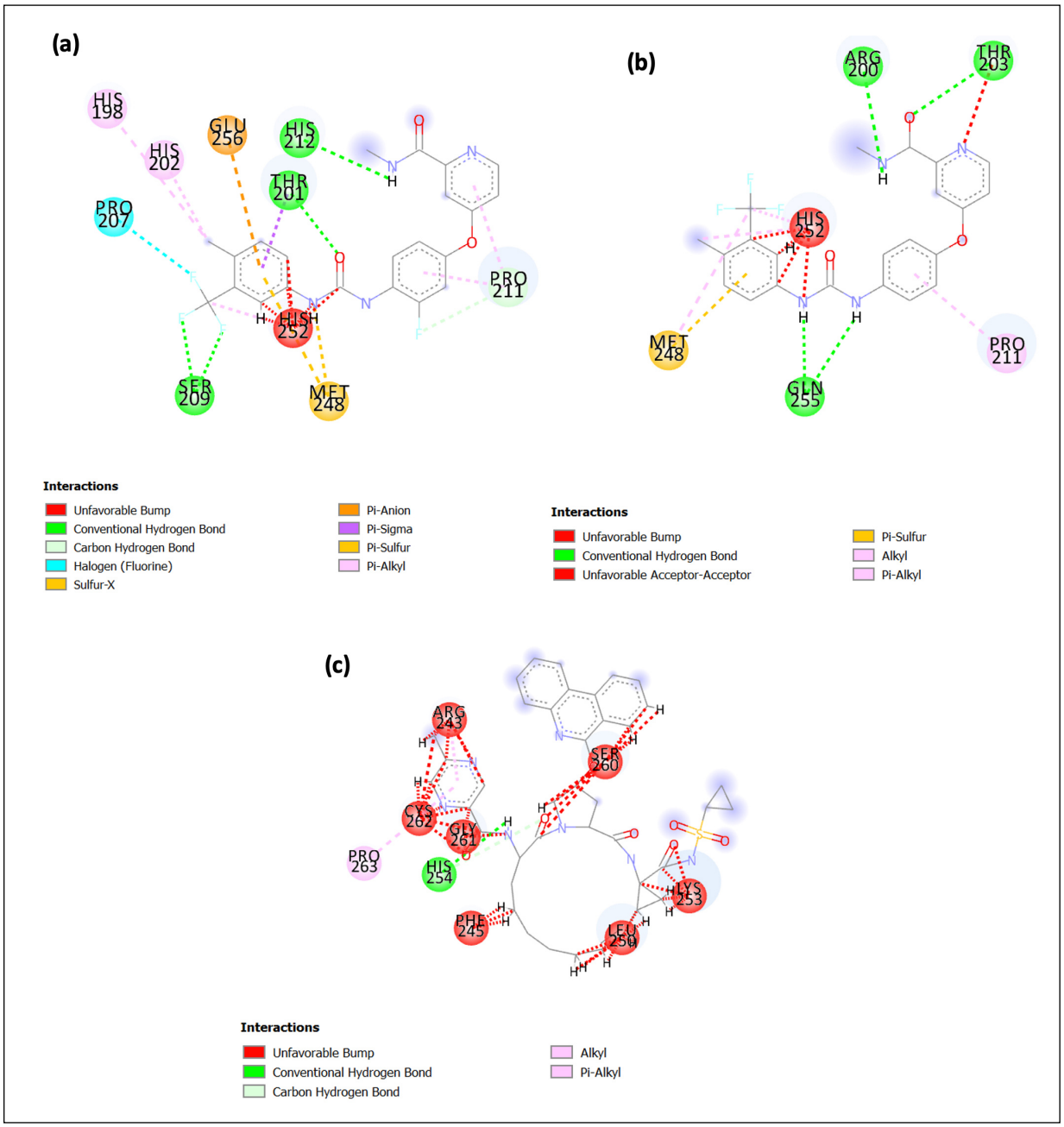

Fig. 3. Interaction of the selected compounds with 3w5k snail protein: Stivarga **(a)**, Sorafenib **(b)**, Paritaprevir **(c)**.

Gln255 for Sorafenib (b), in the substrate binding subsite, leading to strong binding due to hydrogen bonds. Also, Stivarga is accommodated along with the binding site, mainly by π-alkyl interactions with Pro211, His202 and His298. Sorafenib reaches the binding site by π-alkyl interactions with Pro211 and Met248. Unlike these compounds, Paritaprevir (c) binds to the snail protein by one hydrogen bond with His 254, one π-alkyl bond with Pro 263 and several unfavorable interactions with 7 residue of the protein.

Our results are different from those obtained by Li et al[44], who used FTMap, an online computational solvent mapping software (http://ftmap.bu.edu/login.php), to predict the binding hotspots of the protein. They reported that the druggable binding cleft of Snail (PDB id: 3w5k) mainly consists of three main subpockets: R174 pocket, L178 side pocket, and S257 hydrophobic pocket.

Molecular dynamics simulations

Molecular dynamics simulations are of proven *in silico* methods for obtaining dynamic data at atomic spatial resolution[34]. The three compounds

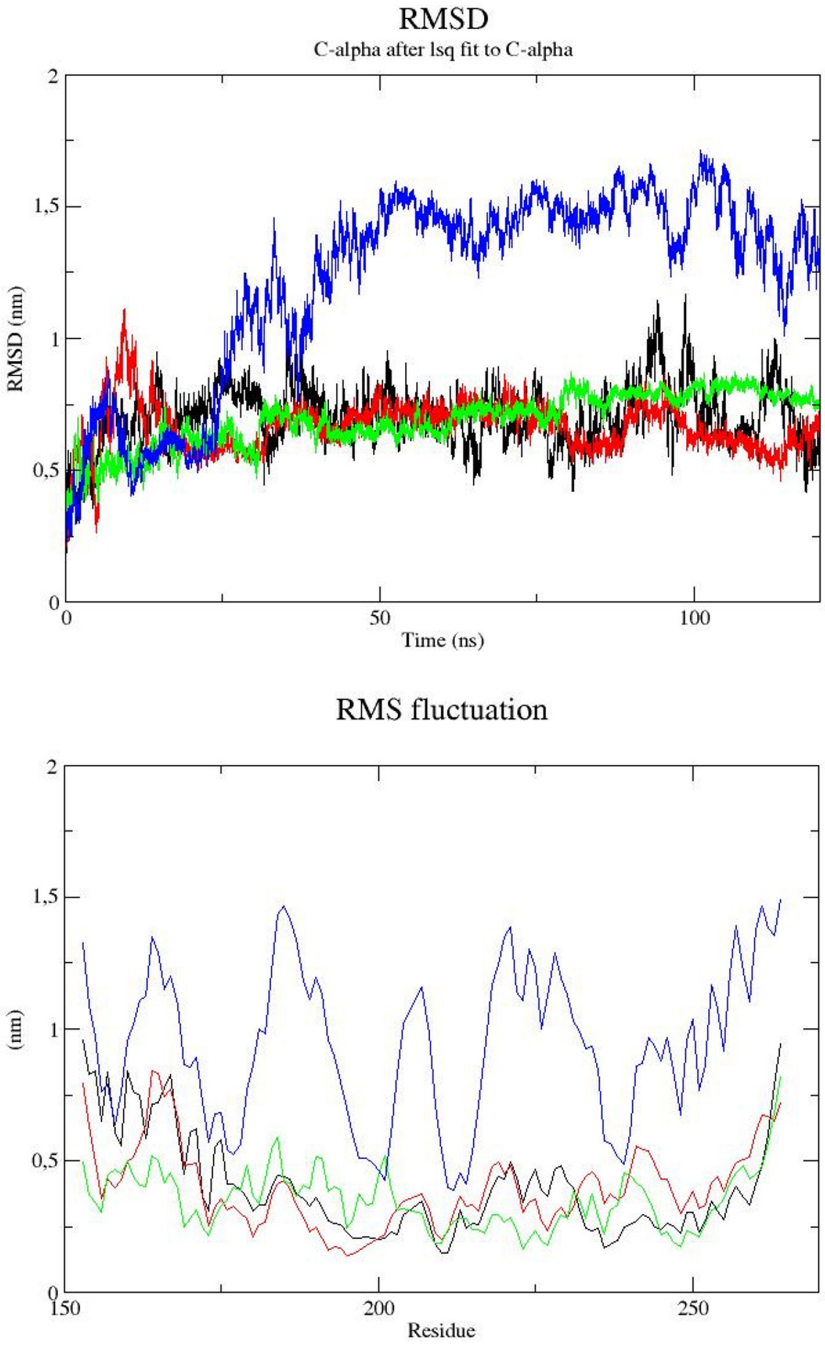

Fig. 4. RMSD and RMSF plots for 3w5k snail protein complex with Stivarga (red), Sorafenib (green) and Paritaprevir (blue) for 120 ns.

with highest scores Stivarga, Paritaprevir and Sorafenib were subjected to MD simulations for 120 ns to analyze the stability of the complexes.

The RMSD evaluated the stability of the complex using the average modification that the protein will undergo during molecular dynamics simulation. The RMSF concerned the structural flexibility by calculating the deviation of the Cα of each residue over time compared to the reference structure (Figure 4).

The differences of backbone RMSD protein in complex with Sorafenib (green) showed the most stable RMSD from 30 ns to 120 ns simulation around 0.75 nm. The Stivarga complex (red) is also stable from 35 ns to 80 ns and constant range of RMSD between 0.75 nm and 0.8 nm. While Paritaprevir complex (blue) was the most instable complex with high RMSD values.

RMSF trajectories provide important information regarding the stability of the complex. High fluctuations in the plot indicate more flexibility and unstable bonds. On the other side, low value or less fluctuation indicates well-structured regions in the complex and less distortion.

As depicted in Figure 4, RMSF of the Sorafenib complex (green) showed low fluctuation from 203 to 220 residues indicating stabilization of protein on this portion. Above 240 up to 264, the protein is stable in the presence of Sorafenib, suggesting that Sorafenib binds to the protein at S257 pocket as described by Li et al[44]. The Stivarga complex (red) showed a fluctuation from 232 to 247 residues and from 154 to 162 (Figure 4).

In order to determine the compactness of the system, Rg was plotted against time. Higher Rg values illustrate less compactness with conformational entropy, while low Rg values are explained as high stability in the structure (more folded). As shown in Figure 5, the Sorafenib complex (green) show less Rg values indicating higher stability around 1.5 nm. While Stivarga and Paritaprévir show higher Rg values revealing less stability.

Hydrogen bonding plays an essential role in determining the binding strength between ligands and 3w5k Snail protein. Sorafenib (green) shows a higher number of hydrogen bonds mostly between 2 and 4 specially after stabilisation (after 30ns) while Paritaprevir complex (blue) showed lower number of hydrogen bonds (Figure 5). Stivarga complex (red) shows similar pattern compared to Sorafenib between 30 and 80 ns. The number of hydrogen bonds contracted between Stivarga and protein decreases after 80ns unlike Sorafenib which showed increased values in the same range of time.

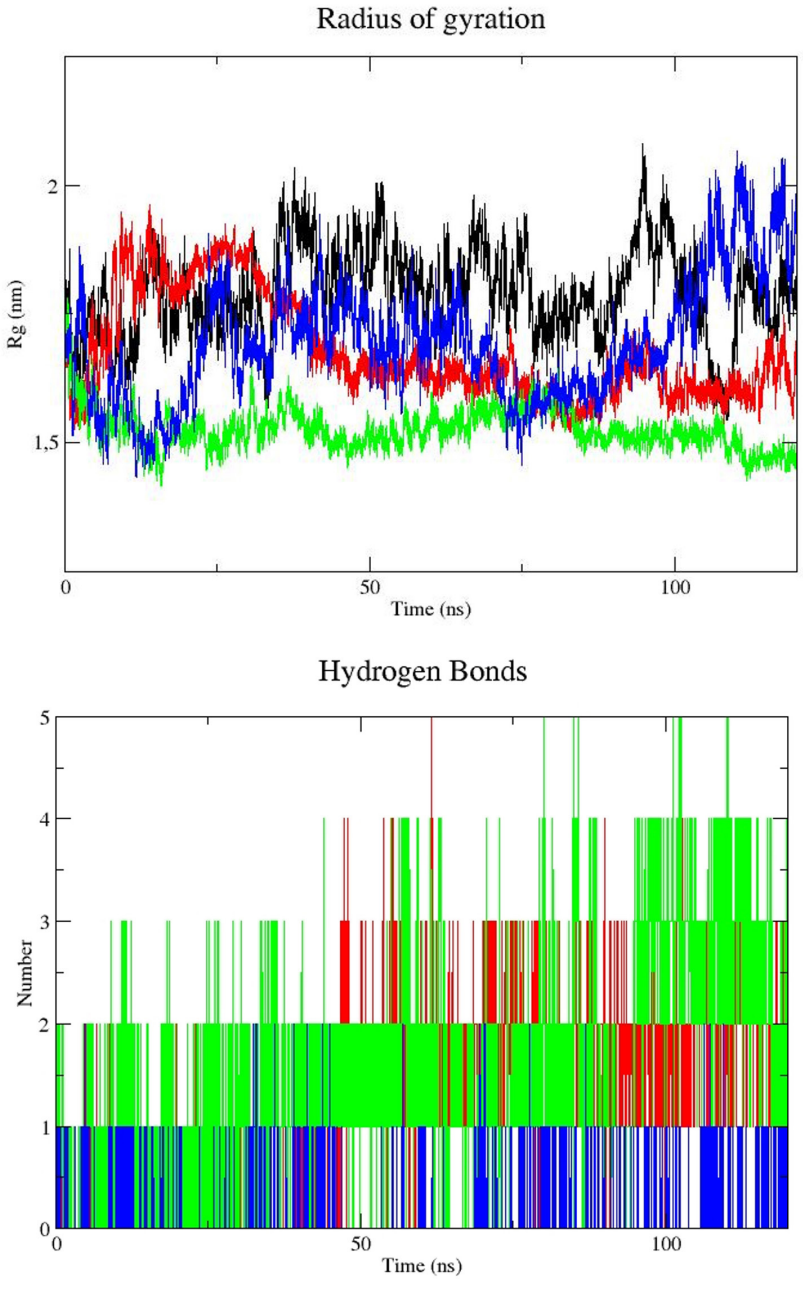

Fig. 5. Rg and hydrogen bonds plots for snail protein complex with Stivarga (red), Sorafenib (green) and Paritaprevir (blue) for 120 ns.

CONCLUSIONS

Compared to other types of cancer, breast cancer recurs more easily and sometimes decades after the initial tumor is removed. The Snail protein is involved in breast cancer metastasis. It constitutes a new prognostic factor and a new therapeutic target.

Through different computational approaches, such as docking studies and molecular dynamics simulations, three approved molecules were identified as potential Snail inhibitors: Stivarga, Sorafenib and Paritaprevir. However, Stivarga and Sorafenib showed better affinity to Snail protein making them potential candidates for simple drug therapies to combat recurrent breast cancer.

Data availability:

All data are available within the manuscript.

Conflict of interest:

The authors have no conflict of interest to report.

Funding:

The author(s) received no specific funding for this work.

Author contributions:

Meriem Benguella-Benmansour: conceptualization, data curation, formal analysis, methodology, writing original draft; Ahmed-Sabri Cherrak: conceptualization, formal analysis methodology, visualization, writing review; Majda Dali-Sahi: conceptualization, methodology, supervision, writing review, validation.

ORCID ID:

Meriem Benguella-Benmansour – https://orcid.org/0000-0003-4746-6927.

REFERENCES

1. Burstein HJ, Curigliano G, Loibl S, Dubsky P, Gnant, M, Poortmans P, Colleoni M, Denkert C, Piccart-Gebhart M, Regan M, Senn HJ, Winer EP, Thurlimann B. Estimating the benefits of therapy for early-stage breast cancer: The St. Gallen International Consensus Guidelines for the primary therapy of early breast cancer 2019. Ann Oncol 2019; 30: 1541-1557.
2. Aguirre-Alvarado C, Segura-Cabrera A, Velázquez-Quesada I, Hernández-Esquivel MA, García-Pérez CA, Guerrero-Rodríguez SL, Ruiz AJ, Rodríguez-Moreno A, Pérez-Tapia SM, Velasco-Velázquez MA. Virtual screening-driven repositioning of etoposide as CD44 antagonist in breast cancer cells. Oncotarget 2016; 7: 23772-23784.
3. Van Denderen BJ, Thompson EW. Cancer: the to and fro of tumor spread. Nature 2013; 493: 487-488.
4. Smolarz B, Nowak AZ, Romanowicz H. Breast Cancer—Epidemiology, Classification, Pathogenesis and Treatment (Review of Literature). Cancers 2022; 14: 2542-2569.
5. Park M, Kim D, Ko S, Kim A, Mo K, Yoon H. Breast Cancer Metastasis: Mechanisms and Therapeutic Implications. Int J Mol Sci 2022; 23: 6791-6806.
6. Williams ED, Gao D, Redfern A, Thompson EW. Controversies around epithelial-mesenchymal plasticity in cancer metastasis. Nat Rev Cancer 2019; 19: 716-732.
7. Wang D, Wang Y, Wu X, Kong X, Li J, Dong C. RNF20 is critical for snail-mediated E-Cadherin repression in human breast cancer. Front Oncol 2020; 10: 613470-613478.
8. Wang Y, Shi J, Chai K, Ying X, Zhou B. The role of snail in EMT and tumorigenesis. Curr Cancer Drug Targ 2013; 13: 963-972.
10. Katoh M, Katoh M. Identification and characterization of human SNAIL3 (SNAI3) gene in silico. Int J Mol Med 2003; 11: 383-388.
11. Peinado H, Olmeda D, Cano A. Snail, Zeb and bHLH factors in tumorprogression: an alliance against the epithelial phenotype? Nature Rev Cancer 2007; 7: 415-428.
12. Choi S, Yamashita E, Yasuhara N, Song J, Son SY, Won YH, Hong HR, Shin YS, Sekimoto T, Park IY, Yoneda Y, Lee SJ. Structural basis for the selective nuclear import of the C2H2 zinc-finger protein Snail by importin β. Acta Crystallographica Section D. Biol Crystall 2014; 70: 1050-1060.
13. Gonzalez DM, Medici D. Signaling mechanisms of the epithelial-mesenchymal transition. Sci Sign 2014; 7: 1-17.
14. Kajita M, McClinic K, Wade PA. Aberrant expression of the transcription factors Snail and Slug alters the response to genotoxic stress. Mol Cell Biol 2004; 24: 7559-7566.
15. Kudo-Saito C, Shirako H, Takeuchi T, Kawakami Y. Cancer metastasis is accelerated through immunosuppression during Snail-induced EMT of cancer cells. Cancer Cell 2009; 15: 195-206.
16. Hsu DS, Wang HJ, Tai SK, Chou CH, Hsieh CH, Chiu PH, Chen NJ, Yang MH. Acetylation of Snail modulates the cytokinome of cancer cells to enhance the recruitment of macrophages. Cancer Cell 2014; 26: 534-548.
16. Zhou BP, Deng J, Xia W, Xu J, Li YM, Gunduz M, Hung MC. Dual regulation of Snail by GSK-3β-mediated phosphorylation in control of epithelial–mesenchymal transition. Nat Cell Biol 2004; 6: 931-940.
17. Knorre DG, Kudryashova NV, Godovikova TS. Chemical and functional aspects of posttranslational modification of proteins. Acta Naturae 2009; 1: 29-51.
18. Liu T, Yu J, Deng M, Yin Y, Zhang H, Luo K, Qim B, Li Y, Wu C, Ren T, Han Y, Lou Z. CDK4/6-dependent activation of DUB3 regulates cancer metastasis through SNAIL1. Nat Commun 2017; 8: 1-12.
19. Zhang K, Rodriguez-Aznar E, Yabuta N, Owen RJ, Mingot JM, Nojima H, Nieto MA, Longmore GD. Lats2 kinase potentiates Snail1 activity by promoting nuclear retention upon phosphorylation. EMBO J 2012; 3: 29-43.
20. Cao YW, Wan GX, Sun JP, Cui XB, Hu JM, Liang WH, Zheng YQ, Li WQ, Li F. Implications of the Notch1-Snail/Slug-epithelial to mesenchymal transition axis for lymph node metastasis in infiltrating ductal carcinoma. Kaohsiung J Med Sci 2015; 31: 70-76.
21. Wu X, Cai J, Zuo Z, Li J. Collagen facilitates the colorectal cancer stemness and metastasis through an integrin/PI3K/AKT/Snail signaling pathway. Biomed Pharmacother 2019; 114: 108708.

22. Du B, Shim JS. Targeting epithelial–mesenchymal transition (EMT) to overcome drug resistance in cancer. Molecules 2016; 21: 965.
23. Kajita M, McClinic KN, Wade PA. Aberrant expression of the transcription factors snail and slug alters the response to genotoxic stress. Mol Cell Biol 2004; 24: 7559-7566.
24. Kurrey NK, Jalgaonkar SP, Joglekar AV, Ghanate AD, Chaskar PD, Doiphode RY, Bapat SA. Snail and slug mediate radioresistance and chemoresistance by antagonizing p53-mediated apoptosis and acquiring a stem-like phenotype in ovarian cancer cells. Stem Cells 2009; 27: 2059-2068.
25. Lu L, Chen Z, Lin X, Tian L, Su Q, An P, Li W, Wu Y, Du J, Shan H, Chiang CM, Wang H. Inhibition of BRD4 suppresses the malignancy of breast cancer cells via regulation of Snail. Cell Death Diff 2020; 27: 255-268.
26. Vistain LF, Yamamoto N, Rathore R, Cha P, Meade TJ. Targeted Inhibition of Snail Activity in Breast Cancer Cells by Using a CoIII-Ebox Conjugate. Chem Bio Chem 2015; 16: 2065-2072.
27. Amawi H, Ashby Jr CR., Samuel T, Peraman R, Tiwari AK. Polyphenolic nutrients in cancer chemoprevention and metastasis: Role of the epithelial-to-mesenchymal (EMT) pathway. Nutrients 2017; 9: 911.
28. Peršurić Ž, Saftić Martinović L, Malenica M, Gobin I, Pedisić S, Dragović-Uzelac V, Kraljević Pavelić S. Assessment of the biological activity and phenolic composition of ethanol extracts of pomegranate (Punica granatum L.) peels. Molecules 2020; 25: 5916.
29. Wishart DS, Feunang YD, Guo AC, Lo EJ, Marcu A, Grant JR. Assempour DrugBank 5.0: a major update to the DrugBank database for 2018. Nucleic Acids Res 2018; 46: 1074-1082.
30. Trott O, Olson AJ. AutoDock Vina Improving the speed and accuracy of docking with a new scoring function, efficient optimization and multithreading. J Comput Chem 2010; 31: 455-461.
31. Dallakyan S, Olson AJ. Small-molecule library screening by docking with PyRx. Humana Press 2015; 1263: 243-250.
32. Kutzner C, Páll S, Fechner M, Esztermann A, de Groot BL, Grubmüller H. More bang for your buck: Improved use of GPU nodes for GROMACS 2018. J Comput Chem 2019; 40: 2418-2431.
33. Abraham MJ, Murtola T, Schulz R, Pa´ ll S, Smith JC, Hess B, Lindahl E. GROMACS: High performance molecular simulations through multi-level parallelism from laptops to supercomputers. SoftwareX 2015; 1: 19-25.
34. Benson NC, Daggett V. A comparison of multiscale methods for the analysis of molecular dynamics simulations. J Phys Chem B 2012; 116: 8722-8731.
35. Yastrebova MA, Khamidullina AI, Tatarskiy VV, Scherbakov AM. Snail-Family Proteins: Role in Carcinogenesis and Prospects for Antitumor Therapy. Acta Nat 2021; 13: 76-90.
36. Grothey A, Prager G, Yoshino T. The mechanism of action of regorafenib in colorectal cancer: A guide for the community physician. Clin Adv Hematol Oncol 2019; 12: S1-S19.
37. Arai H, Battaglin F, Wang J, Lo JH, Soni S, Zhang W, Lenz HJ. Molecular insight of regorafenib treatment for colorectal cancer. Cancer Treat Rev 2019; 81: 101912.
38. Iyer R, Fetterly G, Lugade A, Thanavala Y. Sorafenib: a clinical and pharmacologic review. Exp Opin Pharmacother 2010; 11: 1943-1955.
39. Lesch M, Luckner M, Meyer M, Weege F, Gravenstein I, Raftery M, Sieben C, Martin Sancho L, Imai-Matsuchima A, Welk RW, Frise R, Karlas A. RNAi-based small molecule repositioning reveals clinically approved urea-based kinase inhibitors as broadly active antivirals. PLoS Pathog 2019; 15: 1007601.
40. Shen J, Serby M, Reed A, Lee AJ, Zhang X, Marsh K, Khatri A, Menon R, Kavetskaia O, Fischer V. Metabolism and disposition of the hepatitis C protease inhibitor paritaprevir in humans. Drug Metabol Disp 2016; 44: 1164-1173.
41. Menon RM, Polepally AR, Khatri A, Awni WM, Dutta S. Clinical pharmacokinetics of paritaprevir. Clin Pharmacokin2017; 56: 1125-1137.
42. Brayer SW, Reddy KR. Ritonavir-boosted protease inhibitor based therapy: a new strategy in chronic hepatitis C therapy. Exp Rev Gastroenterol Hepatol 2015; 9: 547-558.
43. Sixto-López Y, Martínez-Archundia M. Drug repositioning to target NSP15 protein on SARS-CoV-2 as possible COVID-19 treatment. J Comp Chem 2021; 42: 897-907.
44. Li HM, Bi YR, Li Y, Fu R, Lv WC, Jiang N, Xu Y, Ren BX, Chen YD, Xie H, Wang S, Lu T, Wu ZQ. A potent CBP/p300-Snail interaction inhibitor suppresses tumor growth and metastasis in wild-type p53-expressing cancer. Sci Advances 2020; 6: 1-17.